# Geoarchaeological and palaeoenvironmental interpretation of residual hills and relict slopes in the Central Ebro Basin, Spain

**José Luis Peña-Monné**
University of Zaragoza: Universidad de Zaragoza
**Maria Marta Sampietro-Vattuone** ( sampietro@tucbbs.com.ar )
National University of Tucuman - CONICET https://orcid.org/0000-0002-7681-070X
**Jesús Picazo-Millán**
University of Zaragoza: Universidad de Zaragoza

**Research Article**

**Keywords:** Holocene, talus flatiron, erosion, geoarchaeology, semiarid environment

**Posted Date:** February 16th, 2022

**DOI:** https://doi.org/10.21203/rs.3.rs-1346394/v1

# Abstract

The cyclical evolution of the testimonial buttes in the central area of the Ebro depression (Los Monegros) is analysed. It is a semiarid environment that favours high erosive rates. The aim of this paper is to obtain an evolutionary model of the Jubierre hills that shows the environmental cycles represented by aggradational and degradative processes on the slopes that produced the present arrangement of talus flatiron rings. In the four studied cases, the talus relicts are composed of detritic material from a disappeared caprock pediment. Four slope stages (S4 to S1) formed under more stable climate conditions are identified. Older stages ages (S4 and S3) are estimated by comparison with other talus flatiron systems from the region. The S2 stage contains Bronze Age archaeological remains and the radiocarbon age obtained was 1608 – 1446 years cal BC (2σ), while S1 is younger. A climate genesis is established for these aggradational stages (S4 to S1). The active erosion of these hills led to a relief inversion and talus flatirons remain as the only features revealing the presence of the old hills and past human occupations.


# 1. Introduction

The central sector of the Ebro depression (NE Spain) underwent a complex and varied geomorphological evolution (Gutiérrez and Peña Monné 1993). Its climate favours semiarid processes and landforms. One of the most outstanding features is the cyclical character of many of the landscape morphologies following environmental changes and human activities (Peña Monné et al. 2000, 2004; Peña Monné 2018). The best expression of these cycles is the evolution of Holocene slopes (Sancho et al. 1988; Gutiérrez et al. 2010, 2015).

The centre of the Ebro depression followed a classic evolution of horizontal or sub-horizontal structures. The incision of the Ebro River and its tributaries produced a fragmentation resulting in plateaus and mesas. The morphologies are characterised by an upper resistant caprock and a weaker talus lower rock that is segmented by minor structural steps (Duszinsky et al. 2019). These landforms progressively evolve to smaller landforms (plateau-mesa-butte-pinnacle) (Migoń et al. 2018, 2019, 2020) through slope retreat. In the final stages, these landforms lost their hard covers to form hills degraded by erosion and badlands (Boroda et al. 2014; Migoń et al. 2018).

In all these stages, but essentially the younger stages, the evolutionary record is only recoverable from the Pleistocene and Holocene talus relicts (talus flatirons) located at various distances from the remaining relief (Sancho et al. 1988; Gutiérrez et al. 2010, 2015; Boroda et al. 2011; Peña-Monné et al. 2019, among others). This type of slope enables us to establish rates for upper scarp retreat (Gutiérrez and Sesé 2001; Boroda et al. 2014; Duszińsky et al. 2019; Oh et al. 2019). Drylands are prone to record this type of landscape evolution given the alternation of contrasting environmental periods (Gerson and Grossman 1987; Schmidt 1994; Gutiérrez et al. 2010; Sheeland and Ward 2018; Peña-Monné al. 2019). There are also dissymmetric talus relict developments related to insolation exposure, especially on Holocene slopes

(Gutiérrez and Peña Monné 1998; Peña Monné et al. 1996), although this dissymmetry may also have structural explanations (Oh et al. 2019).

The aim of this paper is to obtain an evolutionary model and paleoenvironmental interpretation of the residual hills (locally called *tozales)* in the central Ebro Depression (Fig. 1). The environmental cycles is represented by the aggradational and degradative processes in the slopes (talus flatirons) that created the present arrangement of talus flatiron rings. To accomplish this, several hills that are representative of the process were selected and studied using images obtained from sUAV and motion photogrammetry (SfM). The production of high resolution geomorphological maps offers exceptional opportunities to obtain detailed information about these landscapes (Hackney and Clayton 2015; Jorayev et al. 2016). Anthropic features provide chronological and geoarchaeological evidences in several evolutionary stages.

# 2. Geological And Geomorphological Settings

Jubierre is located in the central sector of the Ebro basin (Fig. 1). This tectonic depression is filled with continental sediments accumulated during the Paleogene and Miocene. Paleogeographically, Jubierre is part of the distal section of the “Huesca alluvial fans” (Hirst and Nichols 1986) coming from the Pyrenees. These distal sections are composed of fine detritic lithologies (marls, clays, siltstones, and sandstone channels) and lacustrines (limestones). These latter materials are located towards the south of Jubierre and belong to the Miocene from the Agenian to the Vallesian (Pérez-Rivarés et al. 2003; Pardo et al. 2004) and are part of the Alcubierre Fm (Quirantes 1978). They include the T5 to T7 tectosedimentary units (UTS) of the sedimentary fill of the Ebro basin (Pardo et al. 2004) and are slightly dipped (< 5º) and fractured.

In this region, the Alcanadre and Flumen rivers (Fig. 1) gather the drainage of a large surface of the Pre-Pyrenees and the north side of the Alcubierre mountains. This drainage caused the development of the wide erosive depression of Sariñena on the soft Neogene sediments. The northern sector of the basin is occupied by the fluvial terraces of both rivers, while the south, in the Jubierre area, shows a stepped relief of the Neogene limestones (460–480 m a.s.l.) of the Sierra de Alcubierre up to the fluvial channel of the Alcanadre River (224 m a.s.l.) (Fig. 2). In the south, the upper cornice of the Jubierre sector is formed by limestones, marls, and clays from the Sierra de Pallaruelo-Monte de Sora Unit (Ramírez and Solá Subiranas 1990) (Fig. 3a). Towards the west, lying over the previous Unit, are the limestones of the San Caprasio Unit (Vallesian) in the highest part of the Sierra de Alcubierre (805 m). At the foot of these resistant reliefs are other Miocene Units: Remolinos-Lanaja Unit, Bujaraloz-Sariñena Unit, Galocha-Ontiñena Unit, and Torrente de Cinca-Alcolea de Cinca Unit, arranged from N to S and from most modern to oldest (Salazar and Hernández-Samaniego 1990; Ramírez and Solá Subiranas 1990). The latter are located on the floor valley of the Alcanadre River (220 m) in the northern limit of the study area. All these Miocene Units are composed of marls, siltstones, variously coloured lutites with interbedded sand channels, and lacustrine limestones and marl layers. These all appear deeply eroded (Figs. 3b, 3c, 3d, 3e). The Quaternary evolution of the Jubierre piedmont is characterised by the formation of pediments

produced by successive Pleistocene aggradation and incision phases whose relicts are also included in the present landscape (Fig. 2).

Present climate is continental Mediterranean with semiarid characteristics; annual average precipitations are 470 mm (Sariñena station), with most precipitation falling in spring and autumn (Cuadrat et al. 2007). Mean annual temperature is around 15ºC. Prevailing NW winds (*cierzo*) tend to dry the soils. The area has a significant annual water deficit (-826 mm) that produces poor plant coverage. The structural reliefs are characterised by open forests of quejigos (*Quercus faginea*), holm oak (*Quercus ilex*), sabin juniper (*Juniperus thurifera*), and pine (*Pinus halepensis*), accompanied by scrubs; rosemary (*Rosmarinus officinalis*), thyme (*Thymus vulgaris*), and sage (*Salvia lavandulifolia*). The valley bottom soils are rich in sodium, and so albardín (*Lygeum spartium*) and tamarisk (*Tamarix africana* and *Tamarix gallica*) are abundant near ephemeral water courses.

# 3. Methodology

A detailed terrain survey of the Jubierre area was made by locating several hills with adequate orientation and characteristics for the study of slope successions. Also the hills were selected showing the most complete records including archaeological information for chronological and geoarchaeological purposes. Geomorphological maps were made from spatial datasets (orthoimage and DEM) derived from SfM photogrammetry. Direct field observations were recorded in a Samsung Tab S2 tablet using the QField application for QGIS. Low altitude (60 m) vertical aerial photographs were taken using the sUAV DJI Phantom 4 with a FC220 camera (12.4 Mpx) controlled by a remote controller supporting an Android mobile device. The flight was preconfigured with Pix4DCapture and took 286 photographs (80% overlapped) in two perpendicular grids to improve accuracy covering an area of 0.138 $km^2$. The pictures were processed in Agisoft Metashape Professional v.1.5.1 to obtain an orthomosaic with 2.36 cm/pix ground resolution and a DEM with a 4.72 cm/pix resolution. The DEM was transformed into contour lines, topographic profiles, and a hill-shaded model to enhance the terrain features and estimate the position of landforms to improve mapping.

Highly detailed geomorphological maps from the two selected hills (Los Pedregales N and S) were digitised at 1:468 scale in QGIS v.3.12.2, following the legend proposed by Peña Monné (1997). The detail was necessary due to the dimensions of the hills, surface textures, and the need to highlight the erosive and accumulative landforms. The detailed topographic transverse sections made from the DEM enabled measuring the features related to landscape morphological evolution and these were traced across the slopes corresponding to all evolutionary stages. Another two hills, Solitario1 and Solitario 2, were synthetically studied to complete the information about older stages.

Intensive archaeological surveys were made around the hills. It was possible to recover potsherd sets related to different taluses. These were used to estimate chronologies and their potential source, together with the connections among them. At Los Pedregales S, a small archaeological intervention was made. A 1 m wide front of the talus was cleaned to establish the stratigraphic sequence. One charcoal sample

from this outcrop was dated by 14C AMS by DirectAMS Laboratory (USA). Potsherds were classified and morphometrically and technologically described following the proposal by Picazo (1993) for Bronze Age fragments. The technological study of ceramic pastes followed the usual procedures (cfr. Orton et al. 1993) with the emphasis on inclusions (proportion, shape, and type) and was made with a macroscopic observation followed by microscopic analysis with a 50x digital Dino Lite.

# 4. Results

The Alcanadre River has its head in the Pyrenean External Ranges and reaches the Sariñena depression with N-S orientation. At the confluence with the Flumen River it turns 90º towards the east (Fig. 1) to finally merge with the Cinca River. The Alcanadre River migrated towards the south along the Middle/Upper Pleistocene and constitutes a limit between the smooth relief of the large Quaternary deposits of Sariñena to the north and the abrupt and geomorphologically diverse reliefs of Jubierre towards the south. Calle et al. (2013) identified eight fluvial terraces on the Alcanadre River in the Sariñena depression. Among them, Qt5 is the largest and was dated to 274 – 222 ky BP with ISRL (Rodríguez-Ochoa et al. 2019).

The ephemeral streams coming from the upper limestone reliefs south of the Jubierre descend 260 – 250 m to merge with the Alcanadre River (Fig. 2). These show an average gradient of 5–6%. Their strong erosive power has led to the uphead erosion of the basin (Fig. 3a). There are several levels of Quaternary pediments in the south margin of the Alcanadre River (Fig. 2). These form narrow morphologies dividing the valleys where the main streams flow. These pediments are residual landforms of a large detritic cover and form slightly tilted mesas and testimonial buttes (Fig. 2). The escarpment rim is mainly formed by accumulations of angular limestone fragments coming from the cornices of the Sierra de Pallaruelo-Monte de Sora Unit. These accumulations were formed in several stages and represent periods when high loads were carried by the streams from Jubierre that formed large detritic mantles along the piedmont. At present, incision processes affecting the entire piedmont are dominant and expose the erodible subjacent marls and clays (Fig. 2, 3c). It is sometimes possible to find interbedded resistant layers (sandstones and limestones) in the form of narrow steps with segmented scarps and buttes (Figs. 3d, 3e). Where the resistant layers are eroded, there are only residual hills following a long evolutionary process. The result is a complex labyrinthine landscape that is almost empty of human activity and with a high scenographic value.

# 4.1. Erosive processes in the hills

Many residual hills (*tozales*) are currently very unstable due to erosion caused by several factors. Firstly, their morphology is very abrupt, with slope gradients over 60º. The lack of hard layers on the top of the morphologies, as well as the scarce vegetation cover, offer a wetting front exposed to rain splash (Figs. 3c, 3d, 3e). In addition, the hills develop a steep hydraulic gradient with respect to the drainage base level of the surrounding streams and this leads to high flows with considerable carrying capacity (Benito et al. 1991). Secondly, the lithologies are prone to erosion as they are composed of lutites and marls with

a high content of calcium and sodium sulphates. These are like other lithologies from the Ebro depression where erosion measurements were made by several authors (Gutiérrez et al. 1988, 1997; Benito et al. 1991, 1993; Sirvent et al. 1997). Lastly, the present semiarid climate is characterised by scattered concentrated rains, especially convective storms, during the summer and this magnifies the factors previously mentioned. The variability of this continental Mediterranean semiarid climate is prone to the development of many of the already mentioned processes (Bryan and Yair 1982; Bryan 1987).

The salts contained on marls and clays contribute to haloclasty and hydroclasty – and this increases the weathering processes of the surfaces, together with the dispersive properties of the soils (Jones 1971). The rill subparallel networks are developed from the upper middle sector of the hills (Fig. 3d) with popcorn interills in the lower sections of the hillslope. When intermediate steps are present, it is possible to find conical forms (locally known as “elephant legs”) with gullies and pipes (Figs. 3f, 3g). These surfaces tend to be covered by popcorn morphologies and pedestals (Fig. 3g), and sometimes with large amounts of saline efflorescence. Much of the water flows through piping to reach flat surfaces, such as the structural landings on the base of the hills. As indicated by Jones (1981) and Harvey (1982), piping is the triggering process for the development of these types of rills and gullies. Sediment movement reaches a high level of efficiency by developing silty alluvial fans in the piping outlets as well as surface runoff (Fig. 3f). These environments change quickly and give place to various stages of stepped micro-alluvial fans formed with the silty sediments that are moved through incision cycles. It is usual to find high levels of polygonal cracking density over these silty-clay accumulations. These cracks facilitate rain penetration until they are sealed by sediments or biological soil crusts (Fig. 3h). Biological crusts are formed by lichens and mosses and can temporally slow erosion. These morphologies are shown on the map of Los Pedregales when they are large enough to be represented on our working scale.

We are going to focus on the evolutionary study of the slopes of two of the most geomorphologically interesting hills: Tozales of Los Pedregales North (LPN) and South (LPS) (Figs. 3b, 3c, 3d). Another two hills are also studied for a better documentation of the older slopes: Tozal Solitario 1 (Fig. 3e) and Tozal Solitario 2.

## 4.2. Slope evolution on Tozales de Los Pedregales N (LPN) and S (LPN)

These two hills are in the central sector of Jubierre. Both were formed on the detritic sediments of the Bujaraloz-Sariñena Fm of the Agenian-Aragonian age. They are composed of marls, clays, and siltstones (red, orange, and yellowish). Some narrow layers of lacustrine limestones and sandstones generate largely resistant steps among the soft sediments (Figs. 3c, 3d, 3e). There are also some greyish sandstone paleochannels on the lower section of the accumulations found at the stream incisions, as in the Barranco de la Torre (Figs. 2, 3c). Both hills are located over narrow platforms, the LPS is higher than the LPN (Fig. 4a). These platforms are surrounded by deep incisions produced by the fluvial network. The hills are N-S oriented and clearly visible on the landscape due to their topography and lack of vegetation (Figs. 3b, 3c, 3d).

# 4.2.1. Los Pedregales North (LPN)

The LPN hill has an elongated NNE-SSW shape with a central crest that lacks a resistant upper caprock, and so it can be classified as a residual hill. It is 25 m long and 12 m wide and composed of marls and clays with interbedded thin limestone layers. The water divide is formed by a sharp crest, with 255 m a.s.l. to the SSW and 252 m a.s.l. towards the NNE (Figs. 4a, 4b, 3c). The hilltop is 8 m above the structural platform over which it is located and 27 m above the Barranco de la Torre stream channel. In the geomorphological map (Fig. 5) it is possible to see the isolated position of the hill over the flat structural surface and the steps formed by narrow limestone and sandstone steps descending towards the stream channel. The permanence of the present hill depends on the hardness of these basal structural levels (Figs. 5, 6a, 6b). The main scarp is N-S aligned and its retreat has produced many large blocks that cover part of the slope.

The LPN hill is characterised by the strong erosion produced by microrills and micropiping created by runoff and epidermal flows (Fig. 5). In addition, their stony compositions mean that residual slopes have been preserved. These reliefs have subtriangular shapes, typical of talus flatirons, and feature a high sharpened apex and a smooth reverse (Fig. 5). The deposit is formed by angular clasts of limestone. Two sets of taluses from different ages were identified. They were classified according to their distance from the LPN hill and height, as well as the presence (or absence) of archaeological remains. After classification, considering all the recorded hills from Jubierre, the farthest and therefore oldest slopes from LPN were named S3 and their remains as taluses 6 and 9 in Fig. 5 (see also Figs. 6a). No archaeological remains were found on this stage. The next stage, S2, is younger, closer to the hill than previous stage (S3), and mainly preserved toward the east of the hill (taluses 1 to 5 in Fig. 5) (see also Figs. 6a, 6b). There is also a small relict of S2 on the border of the western scarp (talus 8 in Figs. 5, 6a), and another that is considerably eroded towards the north (talus 7 in Fig. 5).

Most of S2 taluses reveal ceramic Bronze Age potsherds, rolled by transport, among the limestone clasts (Fig. 6a, 6c, 6d). Eighteen ceramic fragments and several flints were recovered from talus 1 (Fig. 5). There are also fragments of mud bricks and mud pavement fragments on taluses 3 and 5, although the quantity was small and the chronological value low. The ceramic fragments recovered from talus 1 belong to small vessels with a fine paste. They were part of open carinated vessels that are typical of the intermediate and late phases of the Bronze Age (second millennia BC; Picazo 1993). A distal section of a flint laminate fits within the proposed chronology. This is also the case of the Genó archaeological sites belonging to the Final Bronze Age (1200 – 1000 cal BC) in the oriental Ebro basin (Maya et al. 1998).

These remains indicate that the hilltop was settled during the slope formation, although there is no *in situ* evidence of archaeological residual materials from the talus. In addition, the remains provide a relative age for stage S2 indicating that it was contemporary or slightly later then Bronze Age.

The location and orientation of the apex enables reconstructing the position of the hilltop and the hill morphology by extending the hillside profile for each slope stage (Fig. 6b). In addition, it was possible to

observe severely weathered sandstone blocks, some of which are large, sparse, and isolated. These had to be part of the hill caprock in some intermediate phase of its evolution. One of these blocks remains in an inclined position lying over the slope deposits. Because of its proximity to the hill, this block is part of the only remains of the S1 stage. It is represented on Fig. 6a (number 10) and on the profile of Fig. 6b.

# 4.2.3. Los Pedregales South (LPS)

The LPS is located over a structural platform above the base of LPN. The hill is 37 m long and 12 m wide, reaching 14 m height at 262 m a.s.l. and is located 34 m above the Barranco de la Torre channel (Figs. 4a, 4b). It is separated from LPN by a pass (and through which much water drains towards the NE) (Fig. 7a). It is geomorphologically more complex than LPN, and on the southern sector it still includes part of a 30 cm thick protective sandstone caprock (Fig. 3d). After a small pass, the hill extends towards the NNE as a descending crest and narrow remains of the S2 stage (talus 8 in Figs. 7a, 7b, 7c). The slope has a steep gradient because it is close to the Barranco de la Torre. It has a stepped appearance because it developed over the sandstone and limestone scarps descending towards the stream channel. It is possible to find clay and marls micro-modelling around the steps produced by rills and piping (Fig. 7a). There are cones, popcorns, vertical mood covers, and micro-pedestals among the piping outlets.

As in LPN, clay layers without a hard protection are exposed in the LPS. The layers are affected by a dense network of microrills and piping (Fig. 7a) with the formation of silty cones at its foot (Fig. 3f). They also show step formations and surficial processes of cracking and biological soil crusts, especially towards the south.

There are remains of older slopes with talus flatiron morphologies. Three evolutionary stages were identified. Two triangular shapes with the apex oriented towards the hill are from the older (S3) stage (taluses 1 and 7 in Figs. 7a, 7c, 8a). These have 0.3–0.4 m thick deposit on the apexes that decrease along the backslope and are composed of angular limestones from the Jubierre – without any material with chronological meaning. The position and orientation of these slopes enables tracing theoretical profiles to locate the paleo escarpment of a higher and larger old hill (Fig. 7c).

Stage S2 is represented by four very eroded taluses, located on the eastern side of the LPS hill (Figs. 7a, 7b, 7c, 8a) with small remains toward the SW (Fig. 7a) on the side of the main scarp (Fig. 7c). There were probably others of the same stage towards the west, but these eroded due to their proximity to the Barranco de la Torre. One of the taluses (talus 5 in Fig. 7a) is oriented in the opposite direction to the rest of the arrangement, and probably belonged to another relief located towards the SE. However, most eastern slopes from stage S2 (taluses 2, 3, 5, and 10 in Figs. 7a, 8a) have ceramic Bronze Age potsherds (the same stage as in LPN), as well as limestone detritic deposits. Thus, they were contemporary or slightly later than the archaeological remains whose source may be in a settlement on the top of the hill that was larger than today.

The most outstanding S2 talus is located toward the north of the hill crest (talus 8 in Figs. 7a, 8a) and it is exceptionally well preserved in the middle section of the butte. This is because there are many

sandstone blocks on its apex protecting an S2 slope that also has a thick and compact deposit. The development of a biological crust also improved its resistance. The most recent slope (S1) is located on the eastern foot of the hill (talus 9 in Figs. 7a, 7c, 8a) and partially lays on an escarpment wall that also contributes to its conservation.

Considering the abundance of ceramic fragments, bones, and charcoals of the S2 (8) relict, a 1 m wide segment of the middle section of the outcrop was cleaned and described (Fig. 8b). The clayey sediments with blocks covering the S2 escarpment together with the head of the S1 slope were removed to access the S2 deposit. Although it is not a primary archaeological site, this is the best approach to learn about the human occupation of the hill over the ages.

The S2 deposit lays over the clays and marls of the Miocene substrate (Fig. 8b). It reaches 120 cm in thickness, towards the left (S) diminishes downslope to 80 cm in thickness. The first unit (A) is composed of yellowish clays with limestone clasts chaotically distributed and whose major axes range between 2 and 10 cm. The unit also contains charcoal fragments. It is followed by Unit B that lays with an inclination of 26º and cuts through the previous unit. Unit B is about 20 cm thick and is composed of reddish clayey sediments with limestone clasts arranged along the inclination of the slope (Fig. 8b). It is a very continuous unit and below the base of the talus. Unit C is 20 cm thick, formed by yellowish silty sediments with the same inclination as the previous unit. It contains bone and charcoal but no ceramic fragments. A charcoal sample was taken (JUB-1) at 30 cm depth close to the contact with the upper unit (D) (Fig. 8b). A dating of 3252 ± 24 BP (1608 – 1446 cal BC, 2σ) was obtained (Table 1). Lastly, Unit D is formed of 20 cm of greyish silts that are completely grey on the top. The surface is covered by an eroded biological crust. Ceramic fragments are more abundant on this upper unit.

The archaeological survey and excavation made on slope 8 of the S2 stage provided ceramic fragments and lithics that resembled the S1 slope located at its foot (talus 9 in Figs. 7a, 8a). The ceramic fragments of S1 are the result of the erosion and sedimentation of the upper slope S2. In general, the ceramics are well preserved and show sharp edges, unaltered surfaces, and are rounded. In addition, a flint flake with thermal cones, a firing pin made over a fluvial quartzite, and bone and charcoal fragments were recovered.

The ceramic set is composed by eight fragments of hand-modelled Bronze Age vessels that were especially common in the middle and late phases. Chronologically they are located between 1700 and 1000 cal BC following comparison other regional studies (Picazo 2005). Among their features, we can highlight the open edges (Fig. 8c) corresponding to middle and small vessels with carinated or S-shaped profiles, with burnished finishes, and fairly good quality pastes. There are three main paste compositions: i) mostly chamotte; ii) mostly quartz; and iii) and mostly mica and quartz. The same materials were recovered from all the taluses showing chronological connections.

Other slopes from the S2 stage arranged as talus flatirons also contain ceramic potsherds as is the case of numbers 3 and 5 (Figs. 7a, 8a). These are smaller and rounded due to the distance from the main hill.

They also have the same paste composition and typologies as those found on slopes 8–9 and the LPN taluses.

The younger S1 stage (talus 9 in Figs. 7a, 8a) is found at the foot of the remains of S2 and contains the materials eroded from the previous stage. The surface of S1 has a stony appearance due to the erosion of fine sediments, but the deposit contains abundant silt and clay together with ceramic fragments like S2. The preservation of the S1 slope may be related with the protection provided by the upper S2 remains. Although in the past it must have covered the entire middle slope and foot of the hill.

### 4.2.4. The slopes in other residual hills

There are many residual hills with talus slopes, although we were unable to locate others with archaeological remains. Another two hills with well-preserved slopes were found that included old stages (S3, S4) that were useful to complete the general evolutionary model. Both *hills* (Tozal Solitario 1 and Tozal Solitario 2) are very close to LPN and LPS. These hills have similar lithological and geomorphological characteristics, although their final morphologies differ.

Solitario 1 is N-S oriented and retains a sandstone layer in the south sector (Figs. 9a, 9b), while the middle to northern area is a narrow clayey crest falling towards the north. This hill presents old slopes from past stages (S4 and S3) that are especially large on the west side (Figs. 9a, 9b). As in LPN and LPS, among the limestone clasts of the slope S2 (Fig. 9c) a Bronze Age potsherd was located (Fig. 9d).

Solitario 2 is a clayey hill with a sandstone caprock and completely lacks vegetation. It is deeply affected by rills and piping located above a thick sandstone platform over which the cones of silt and gravels carried by the rills descending from the hill wall are deposited (Figs. 10a). Two S3 slopes are preserved while the S2 talus ring is completely preserved except towards the eastern hill face (Figs. 10a, 10b). Three large ceramic fragments, perhaps of the same vase were found at one of the talus flatiron of the S2 stage (Figs. 10a, 10c). These potsherds (Fig. 10d) show similar thickness, finish, and inclusions of those already described belonging to the Bronze Age, although they present rounded edges. Solitario 2 also retains a small talus closer to present hill from S1 stage (Fig. 10a, 10b).

## 5. Discussion

## 5.1. The geomorphological arrangement and the hills formation

The four hills analysed have the same lithological composition and are part of the same starting geomorphological arrangement. The lutites and marls of the Bujaraloz-Sariñena and Galocha-Ontiñena Units (Agenian- Aragonian) unit are very erodible, despite the interbedded sandstones and limestones. At present, piping and runoff (rills and gullies) evidence high erosion rates for the Miocene materials. Along the Quaternary, the Alcanadre River represented the general base level of the drainage network of Jubierre. The aggradational, stabilisation, and incision phases of the floodplain determined the

aggradative/degradative dynamics of the Jubierre tributaries. The result was the formation of pediment stages with gradients oriented towards successive fluvial levels. Thus, at the beginning of the process there was a good connection between pediments and fluvial terraces. The fluvial network of Jubierre is formed by steep ephemeral streams, flowing in parallel towards the Alcanadre River. The confluence of these streams is perpendicular to the Alcanadre River because it turns east after merging with the Flumen River (Figs. 1, 2).

The detrital cover of the pediment phases, with thicknesses of 2–6 m, is preserved in the upper section of the numerous reliefs located on the middle and lower sectors of Jubierre (Fig. 2). They form mesas and residual hills at various altitudes (Fig. 11). These reliefs also form water divides among the water courses deeply entrenched on the soft Miocene materials. Thus, their morphologies are S-N oriented. The arrangement of parallel S-N drainage networks and intermediate reliefs is still present.

The evolutionary process evidenced by the residual slopes is the result of the erosive retreat of the intermediate reliefs in all the margins. This is particularly evident on E and W slopes. These margins are highly dynamic due to the nearness of lateral streams. Therefore, the resulting reliefs are narrow and S-N elongated.

Another important factor is the insolation exposure. In our study cases, it is not possible to find much contrast among the slope development. This is because we chose subelliptic hills with small N and S slopes. The orientation factor produces notable differences in incident energy and the humidity available to maintain a protective plant cover. It also influences the capacity for recuperation after fire, overgrazing, and other human activities (Burillo et al. 1981; Burillo and Peña Monné 1984). This promotes the development of dissymmetric hills (Peña Monné et al. 1996) because erosion is greater on southern slopes (Northern Hemisphere). However, north-facing slopes can be more stable and even insensitive to environmental changes, especially during the Holocene (Peña Monné 2018).

The taluses of our studied hills are composed of limestone gravels and boulders. This litologies are only present on the Pleistocene pediments from Jubierre and the high Miocene limestone corniches of the Sierra de Alcubierre. This enables us to infer that the caprock of all hills was a detrital cover of pediment. This type of material is currently identifiable *in situ* on the hilltop of less evolved hills from Jubierre (Figs. 2). These top deposits are cemented by carbonates that have become resistant calcretes (Sancho and Meléndez 1992; Meléndez et al. 2011). These detrital levels were represented in the cross-sections (Figs. 6b, 7b, 7c; 9b, 10b) in the inferred past positions. Their positions and altitudes were estimated from nearby reliefs that still retain these covers together with inclined taluses. We estimate that the same pediment level covered LPN, LPS, and Solitario 1 and Solitario 2 probably had a higher -and then older- pediment.

Many reliefs from Jubierre have Quaternary pediments on their tops, but it is difficult to establish stages because they are small and disconnected from each other (Fig. 2). Four stages were identified in the topographic cross-section (Fig. 11) drawn between the southern limestone platforms (Sierra de Alcubierre) and the Alcanadre River (N), although there are some higher remains. The theoretical surface

level was reconstructed through the platform surfaces up to the Alcanadre River as a base level to enable establishing these surfaces at 90–100, 55–60, 30–35, and 10–12 m above the present river channel (Fig. 11). The fluvial terraces of the Alcanadre River in the Sariñena area are located at 180 m (Qt1), 120 m (Qt2), 55 m (Qt3), 30 m (Qt4), 20–25 m (Qt5), 25 m (Qt6), 10 m (Qt7), and 3–5 m (Qt8) above the present channel (Calle et al. 2013). These relative heights enable us to consider possible relationships between the 90–100 m pediment and Qt2 terrace, that of 55–60 m with Qt3, that of 30–35 m with Qt4 or Qt5, and that of 10–12 m with Qt7. Considering the fluvial terraces of the left margin of the Alcanadre River (there are no terraces preserved on the right margin) the most topographically probable pediment related to the LPN, LPS, and Solitario 1 hilltops is that of 30–35 m (Fig. 11) and this could be connected with Qt4 or Qt5 fluvial terraces. The Qt5 was dated by OSL between 196 ± 13 y 274 ± 18 ky (Rodríguez-Ochoa et al. 2019). Solitario 2 top may be the pediment connected with Qt3 or Qt4 terraces and older than the other hills. However, this is difficult to establish without direct datings.

In the reconstruction of Fig. 12a pediment was represented as the starting landform for the evolution of these hills without establishing an age. From the progressive retreat of the upper scarp, successive phases of stabilisation or incision were established on the slopes. This process is represented in Figs. 12a to 12e and was accompanied by the intense incision of the surrounding ephemeral streams as the hills shrank. The detrital caprock loss was sustained up to the S2 stage on the four hills analysed because the eroded materials are found on the S4, S3, and S2 stages. The younger stage (S1) is present in LPS and composed of the materials eroded from S2 on which it sits. There are small remains of this stage in LPN and Solitario 2.

After the erosion of the upper detrital caprock (Figs. 12d, 12e), it was replaced as the erosion advanced by lower sandstone and limestone layers, as in Solitario 1 (Fig. 3e, 9a), Solitario 2 (Fig. 10a, 10b), and LPS (Fig. 3d, 7a), and so the erosive process slowed. In other cases, the upper protection was totally lost such as on LPN and most of LPS and Solitario 1. This is critical because no other hard Miocene layers are visible. Thus, it will erode quickly.

According to this evolutionary interpretation (we avoid to mention the talus flatiron usually preserved), present hills (*tozales*) from Jubierre might be on different evolutionary stages. This permits to classify these hills into three groups (Fig. 13). The less evolved, the mesas (1) and conical hills (2), still have a caprock formed by the cemented calcareous gravels of the Pleistocene pediments; they a followed by the buttes that loss the detrital caprock but retain other caprocks formed by resistant lithologies (especially sandstones) lying on lower positions than the cemented gravels (4). The scarp retreats gave place to the development of monolithic shapes and pinnacles (5). Finally, after loss any resistant layer, the hill become small mounds modeled on marls and clays shaped as convex hills (5a) or conical hills and sharp crests (5b). The fast erosion of these hills form badlands and residual reliefs with scattered blocks of the old caprocks (6).

# 5.2. Talus flatirons stages and interpretation

The relict talus slope or talus flatirons surround the hills as concentric rings – such as those described by Morgan et al. (2008) and Gutiérrez et al. (2015) in Colorado (USA). They are a record of the slopes that enable us to interpret and reconstruct the evolution of the hills. Flatirons develop in various climatic environments and are common in drylands, such as the Tertiary depressions in NE Iberia. There are many publications about talus flatirons in the Ebro depression (Sancho et al. 1988; Arauzo et al. 1996; Gutiérrez et al. 1996, 1998a, 1998b; Gutiérrez and Peña Monné 1998), as in the Duero (Gutiérrez and Sesé 2001) and Tagus depressions (Peña-Monné et al. 2019), together with regional perspectives (Gutiérrez et al. 2003, 2006, 2010).

The talus flatirons developed in Israel during the Quaternary, as shown by cosmogenic nuclide exposure datings ($^{10}$Be) for the Middle Pleistocene (around 610, 550, and 270 ky) (Boroda et al. 2011, 2013). A stage of > 124 ky dated by OSL was established by Gutiérrez et al. (2015) in the Colorado piedmont (USA). The oldest talus flatiron in the Iberian Peninsula is found in the Teruel depression, dated to 152 ± 17 ky with OSL (Peña-Monné et al. 2022). Intermediate ages are more frequent, and in the Iberian Peninsula such flatirons have been described towards the NE of the Henares River basin and dated to *ca.* 88 ky *ca.* and 56 ky (there are two older stages without datings) (Peña-Monné et al. 2019). However, the Upper Pleistocene and Holocene phases from the Tertiary basins of NE Iberia (Ebro, Duero, and Tagus) are better known (Gutiérrez et al. 1996, 2003, 2006, 2010). Until now, four phases were established with ages from oldest to youngest around 36–41 ky (S4), 28–30 ky (S3), 3.6–2.5 ky (S2) and 1 ky (S1).

Although it is not possible to date the coarse detrital materials of the S4 and S3 stages, can be assumed a chronological relationship with the stages defined by Gutiérrez et al. (2010) at around 36–41 ky and 28–30 ky respectively. The spatial vicinity among S4 and S3 stages in the Solitario1 and Solitario 2 hills could be related to their chronological proximity. The only slopes in Jubierre with a dating are the S2. Several S2 talus preserved in the four hills analysed include ceramic potsherds from the Bronze Age and were radiocarbon dated in LPS to 1608 – 1446 cal BC (Middle Bronze Age). This suggests the chronological coincidence with the S2 phase determined by other already cited authors. This type of geoarchaeological relationship with a talus flatiron phase was established in various archaeological sites by Burillo et al. (1981, 1983), Peña Monné and González (1992), Peña Monné and Rodanés (1993), Peña Monné et al. (1996, 2005, 2019), Pérez-Lambán et al. (2014), and Peña Monné (2018). The information provided by these papers shows that this talus flatiron stage was developed from the end of the Chalcolithic (4200 BP) up to the Iron Age (700 – 500 BP). It was related with a humid and relatively cold phase whose climax was the Iron Age Cold Phase or 2.8 event (Bond et al. 1997). The stage S1 was geoarchaeologically defined, but more accurate datings point to the existence of two aggradative phases during the Little Ice Age (Pérez-Lambán et al. 2014; Peña Monné 2018). Although we do not have dating from Jubierre, this phase is represented by small remains from LPN, LPS and Solitario 2.

Human occupations occurred on LPN and LPS during the S2 stage around 3500 ago, when the detrital caprock was still on the hilltop (Fig. 11c). In addition, its contemporary talus is separated from the present hill by between 10 and 25 m. This implies a large volumetric loss. These types of estimations are difficult for the older stages, especially without dating. However, accepting the dating for other areas of

the Ebro depression, the stage retreats for S4 and S3 were relatively slow and this was probably due to caprock protection. From the archaeological point of view, the recent erosive acceleration quickens the loss of many archaeological sites located in high places, mainly from Bronze Age, Iron Age, and Iberian Epoch. This implies a problem for the reconstruction of the peopling of these semiarid environments due to an information loss that is only recoverable by geoarchaeological techniques (Peña Monné 2018).

In general, the evolutionary dynamic of the hills at Jubierre show a predominance of degradative processes, together with the entrenchment of the surrounding ephemeral streams. The development of slopes with thick accumulations of sediments reflects interruptions of the generalised erosive process. Stable periods with cold and wet climatic events point to a climatic cause for these events. The degradative dynamics are recovered with the re-establishment of 'normal' dry and warm conditions, as is the case of the present situation. This is, according to references, the most accepted explanation for the formation of S2 and S1 stages, as well as for the intermediate incision phases. However, older stages are more difficult to connect with global climatic phases (Gutiérrez et al. 2006, 2010; Boroda et al. 2015). It is more feasible to relate them with regional cold phases, such as the old phases of the Henares valley (Tagus basin) (Peña-Monné et al. 2019) or the Teruel depression (Iberian Ranges) (Peña-Monné et al. 2022) related with the glacial phases recorded in the Pyrenees.

Another variable for the Holocene stages is the possible addition of anthropic influence as a new active factor normally triggering or increasing degradative processes. The accumulations remaining from those erosive processes are mainly silts located on the valley floors from Jubierre (Holocene infills in Fig. 2) Results obtained in the Ebro basin show that valley fills started due to slope erosion produced by deforestation and beginning at the Neolithic. Sedimentation rates increased with the Bronze Age in some areas and are especially rapid in the Iberian and Roman Epochs (3rd century BC to 5th century AD) (Constante et al. 2010; Peña Monné et al. 2000, 2004, 2018, Peña Monné 2018). Average sedimentation rates of 4.5 m/kyr were calculated for that period (Peña-Monné and Sampietro-Vattuone 2019). In conclusion, the incision produced over the S2 slope occurred during the warmer and drier period of the beginning of the Subatlantic but was accelerated by human influence. These double climatic/anthropic factors are also possible causes of the S1 stage degradation during the Warm Present Period.

# 6. Conclusions

The evolution of the Jubierre reliefs is the consequence of the conjunction of semiarid conditions at the centre of the Ebro depression and the dominant lithologies. The presence of several stages of talus relict (talus flatirons) generated under other environmental conditions are the best record of a complex evolution. Wetter periods from the Upper Pleistocene and Holocene gave rise to stable phases on the slopes with aggradative taluses in the hills. It is possible to identify at least four phases (S4 to S1). Intermediate incision periods isolated each talus set and these remain separated from the upper caprock following an erosive retreat. Finally, each talus set remained arranged as concentric rings around the main hill.

The arrangement of the taluses, their composition, gradient, distance to the hills, and inferred morphologies enable a reconstruction of the characteristics, size, height, and position of the original caprock. Between S4 and S2 stages, the hills maintained similar detrital caprocks (Pleistocene pediments). The scarce remains of the S1 stage show that the caprock was already eroded.

Stage S2 in the four hills analysed is the most interesting due to the human remains that are contemporary to its formation. Ceramic potsherds, and the radiocarbon dating enable us to establish that it was formed during the Middle Bronze Age. Geoarchaeologically, it is necessary to highlight the importance of these taluses as the last remaining records for reconstructing old human occupations in these environments.

# Declarations


### Acknowledgements

This work is a contribution of the “Primeros pobladores y Patrimonio Arqueológico del Valle del Ebro” Aragon Research Group (Government and European Regional Development Fund). This work has partially benefited from financial and technical support provided by the projects CLIP HAR2014-59042-P and HAR2015-65620-P, provided by the Spanish Inter-Ministry Commission of Science and Technology (CICYT); and PICT2018-1119, PICT2019-0931, and PIUNT G629. This paper is within the research scope of IUCA (Environmental Sciences Institute of the University of Zaragoza).

### Funding

This work was supported by the Spanish Inter-Ministry Commission of Science and Technology (CICYT) (CLIP HAR2014-59042-P and HAR2015-65620-P), the Agencia Nacional de Promoción Científica y Tecnológica (PICT2018-1119 and PICT2019-0931), and the Universidad Nacional de Tucumán (PIUNT G629).


### Competing Interests

The authors have no relevant financial or non-financial interests to disclose.

# References


1. Arauzo T, Gutiérrez M, Sancho C (1996) Facetas triangulares de ladera como indicadores paleoclimáticos en ambientes semiáridos (Depresión del Ebro). Geogaceta 20(5):1093-1095
2. Benito G, Gutiérrez M, Sancho C (1991) Erosion patterns in rill and interrrill areas in badlands zones of the middle Ebro Basin (NE-Spain). In: Sala M,  Rubio JL, GarcíaRuiz JM (eds) Soil Erosion Studies in Spain. Geoforma Ediciones, Madrid, pp. 41-54
3. Benito G, Gutiérrez M, Sancho C (1993) The influence of physico-chemical properties on erosion processes in badland areas, Ebro basin, NE Spain. Z. Geomorphol. N.F. 37:199-214

4. Bond G, Showers W, Cheseby M, Lotti R, Almasi P, deMenocal P, Priore P, Cullen H, Hajdas I, Bonani G (1997) A pervasive millennial-scale cycle in North Atlantic Holocene and glacial climates. Science 278:1257-1266
5. Boroda R, Amit R, Matmon A, Finkel R, Porat N, Enzel Y, Eyal Y (2011) Quaternary-scale evolution of sequences of talus flatirons in the hyperarid Neguev. Geomorphology 127:41-52. https://doi.org/10.1016/j.geomorph.210.12.003
6. Boroda R, Matmon A, Amit R, Haviv I, Porat N, ASTERTeam, Rood D, Eyal Y, Enzel Y (2013) Long-term talus flatirons formation in the hyperarid northeastern Negev, Israel. Quaternary Research 79(2):256-267.
7. Boroda R, Matmon A, Amit R, Haviv I, Arnold M, Aumaître G, Bourlès DL, Keddadouche K, Eyal Enzel Y, Yehouda E (2014) Evolution and degradation of flat-top mesas in the hyper-arid Negev, Israel revealed from 10Be cosmogenic nuclides. Earth Surf. Process. Landf. 39:1611-1621
8. Boroda R, Matmon A, Amit R, Haviv I, Porat N, ASTER Team, Rood D, Eyal Y, Enzel Y (2015) Long-term talus flatirons formation in the hyperarid Negev, Israel. Quaternary Research 79:256-267. http://dx.doi.org/10.1016/j.yqres.2012.11.012
9. Bryan R (1987) Processes and significance of rill development. Catena Suppl. 8:1-15.
10. Bryan RB, Yair A (1982) Perspectives on studies of badland geomorphology. In: Bryan R, Yair A (eds.) Badland Geomorphology and Piping. Geobooks, Norwich, pp. 1-12
11. Burillo F, Gutierrez M, Peña Monné JL (1981) El Cerro del castillo de Alfambra (Teruel). Estudio interdisciplinar de Geomorfología y Arqueología. Kalathos 1:7-63
12. Burillo F, Gutiérrez M, Peña Monné JL (1983) La Geoarqueología como ciencia auxiliar. Una aplicación a la Cordillera Ibérica Turolense. Revista de Arqueología 26:6-13
13. Burillo F, Peña Monné JL (1984) Clima, geomorfología y ocupación humana. Introducción a un planteamiento metodológico. In: Actas Iª Jornadas de Metodología de Investigación Prehistórica, Soria, pp. 91-102
14. Calle M, Sancho C, Peña JL, Cunha P, Oliva-Urcía B, Pueyo E (2013) La secuencia de terrazas cuaternarias del río Alcanadre (provincia de Huesca): caracterización y consideraciones paleoambientales. Cuad. Invest. Geográficas 39(1):159-178. http://dx.doi.org/10.18172/cig.2004
15. Constante A, Peña-Monné JL, Muñoz A (2010) Alluvial geoarchaeology of an ephemeral stream: Implications for Holocene landscape change in the Central part of the Ebro Depression, Northeast Spain. Geoarchaeology 25(4):475-496. http://dx.doi.org/10.1002/gea.2031
16. Cuadrat JM, Saz Sánchez MA, Vicente SM (2007) Atlas climático de Aragón. Gobierno de Aragón, Zaragoza
17. Duszyński F, Migoń P, Strzelecki MC (2019) Escarpment retreat in sedimentary table-lands and cuesta landscapes – Landforms, mechanisms and patterns. Earth Sci. Rev. 196:102890. https://doi.org/10.1016/j.earscirev.2019.102890
18. Gerson R, Grossman S (1987) Geomorphic activity on escarpments and associated fluvial systems. In: Rampino MR, Sanders JE, Newman WS, Königsson LK (eds) Climate, History, Periodicity and

Predictability. Reinhold, New York, pp. 300-322

19. Gutiérrez F, Morgan ML, Matthews V, Gutiérrez M, Jiménez-Moreno G (2015) Relict slope rings and talus flatirons in the Colorado Piedmont: Origin, chronology and paleoenvironmental implications. Geomorphology 231:146-161. https://doi.org/10.1016/j.geomorph.2014.11.024
20. Gutiérrez M, Gutiérrez F, Desir G (2003) Are talus flatirons from Central Spain related with Heinrich events? Suppl. Geogr. Fis. Dinam. Quat. 6:59-63
21. Gutiérrez M, Gutiérrez F, Desir G (2006) Considerations of the chronological and causal relationships between talus flatirons and palaeoclimatic changes in central and northeastern Spain. Geomorphology 73:50-63
22. Gutiérrez M, Lucha P, Gutiérrez F, Moreno A, Guerrero J, Martín-Serrano A, Nozal F, Desir G, Marín C, Bonachea J (2010) Are talus flatiron sequences in Spain climate-controlled landforms? Zeitschrift für Geomorphologie 54:243-252. https://doi.org/10.1127/0372-8854/2010/0054-0013
23. Gutiérrez M, Peña Monné JL (1998) Geomorphology and Late Holocene climatic change in northeastern Spain. Geomorphology 23:205-217.
24. Gutiérrez M, Sancho C, Arauzo T (1998a) Cliff retreat rates in semiarid environments from talus flatirons, Ebro Basin, NE Spain. Geomorphology 25:111-121. https://doi.org/10.1016/S0169-555X(98)00034-8
25. Gutiérrez M, Arauzo T, Sancho C, Peña-Monné JL (1998b) Evolution and paleoclimatic meaning of the talus flatirons in the Ebro Basin, northeast Spain. In: Alsharhan AS, Glennie KW, Whittle GL, Kendall CG (eds) Quaternary Deserts and Climatic Change. Balkema, Rotterdam, pp. 593-599
26. Gutiérrez M, Sancho C, Arauzo T, Peña-Monné JL (1996) Talus flatirons as indicators of climatic changes in a semiarid región (Ebro Basin, Spain). In: Benito G, Pérez-González A, Machado MJ, de Alba S (eds) Palaeohydrology in Spain. Toledo, Spain, pp. 35-44
27. Gutiérrez M, Sesé VH (2001) Multiple talus flatirons, variations of scarp retreat rates and the evolution of slopes in Almazán Basin (semi-arid central Spain). Geomorphology 38:19-29. https://doi.org/10.1016/S0169-555X(00)00051-9
28. Gutiérrez M, Sancho C, Benito G, Sirvent J, Desir G (1997) Quantitative study of piping processes in badland areas of the Ebro Basin, NE Spain. Geomorphology 20:237-253
29. Gutiérrez M, Benito G, Rodríguez J (1988) Piping in badland areas of the middle Ebro basin, Spain. Catena Suppl. 13:49-60
30. Hackney Ch, Clayton A (2015) Unnamed Aerial Vehicles (UAVs) and their application in geomorphic mapping. In: Cook S, Clarke L, Nield J (eds) Geomorphological Techniques, chap. 2, sec. 1.7, British Soc. for Geomorphology, London, pp. 1-12
31. Harvey A (1982) The role of piping in the development of badlands and gully systems in South-East Spain. In: Bryan RB, Yair A (eds) Badlands geomorphology and piping. Geobooks, Norwick, pp. 317-35
32. Hirst JPP, Nichols GJ (1986) Thrust tectonic controls on Miocene alluvial distribution patterns, southern Pyrenees. In: Allen P, Homewood P (eds) Foreland Basins. International Association of

Sedimentologist Special Publications (8), Washington, pp. 247-258

33. Jones JAA (1981) The Nature of Soil Piping. Res. Monogr. Ser. 3, GeoBooks, Norwich, 301 pp
34. Jones JAA (1971) Soil piping and strearn cbannel iniciation. Water Resources Research 7(3):602-610
35. Jorayev G, Wehr K, Benito-Calvo A, Njau J, de la Torre I (2016) Imaging and photogrammetry models of Olduvai Gorge (Tanzania) by Unmanned Aerial Vehicles: A high-resolution digital database for research and conservation of Early Stone Age sites. Journal of Archaeological Science 75:40-56
36. Maya JL, Cuesta F, López Cachero J (eds) (1998) Genó: Un poblado del Bronce final en el Bajo Segre (Lleida), Universitat de Barcelona, Barcelona
37. Meléndez A, Alonzo-Zarza AM, Sancho C (2011) Multi-storey calcrete profiles developed during the initial stages of the configuration of the Ebro Basin's exorrheic fluvial network. Geomorphology 134:232-248
38. Migoń P, Różycka M, Jancewicz K, Duszyński F (2018) Evolution of sandstone mesas following landform decay until death. Prog. Phys. Geogr. 42:588-606
39. Migoń P, Duszyński F, Jancewicz K, Różycka M (2019) From plateau to plain – using ergodic assumption in interpreting geoheritage through a thematic trail, Elbsandsteingebirge, Germany. Geoheritage 11:839-855.
40. Migoń P, Duszyński F, Jancewicz K, Kotwicka W (2020) Late evolutionary stages of residual hills in tablelands (Elbsandsteingebirge, Germany). Geomorphology 367:107308. https://doi.org/10.1016/j.geomorph.2020.107308
41. Morgan ML, Matthews V, Gutiérrez F, Thorson JP, Madole RF, Hanson PR (2008) From buttes to bowls: Repeated relief inversión in the landscape of the Colorado Piedmont. In: Raynolds RG (ed) Roaming the Rocky Mountains and Environs. Geological Field Trips. The Geological Soc. of America, Field Guides, 10, pp. 203-215
42. Oh JS, Seong YB, Larson PH, Hong SC, Yu BY (2019) Asymmetric Hillslope Retreat Revealed from Talus Flatirons on Rock Peak, San Tan Mountains, Arizona, United States: Assessing Caprock Lithology Control on Landscape Evolution. Annals of the American Association of Geographers 110(1):98-119. https://doi.org/10.1080/24694452.2019.1624421
43. Orton C, Tyers P, Vince A (1993) Pottery in Archaeology. Cambridge University Press, Cambridge
44. Pardo G, Arenas C, González A, Luzón A, Muñoz A, Pérez A, Pérez-Rivarés FJ, Vázquez-Urbez M, Villena J (2004) La cuenca del Ebro. In: Vera JA (ed) Geología de España. IGME and Sociedad Geológica de España, Madrid, pp. 533-543
45. Peña Monné JL (1997) Cartografía geomorfológica básica y aplicada. Ed. Geoforma, Logroño, 235 pp
46. Peña Monné JL (2018) Geoarqueología aplicada a la reconstrucción paleoambiental: La evolución del Holoceno superior en el NE de España. Boletín Geológico y Minero 129(1/2):285-303, http://doi.org/10.21701/bolgeomin.129.1.011

47. Peña-Monné JL, Cunha P, Sampietro-Vattuone MM, Bridgland DR, Murray AS, Buylaert JP (2022) The connections between river terraces and slope deposits as paleoclimate proxies: The Guadalaviar - Turia sequence (Eastern, Iberia Chain, Spain). Global and Planetary Change 208: 103728. https://doi.org/10.1016/j.gloplacha.2021.103728
48. Peña Monné JL, González JR (1992) Hipótesis evolutiva de los cambios en la dinámica geomorfológica del Baix Cinca y Segre (Depresión del Ebro) durante el Pleistoceno superior-Holoceno a partir de los datos geoarqueológicos. Cuaternario y Geomorfología 6:103-110.
49. Peña Monné JL, González Pérez JR, Rodríguez Duque JI (1996) Paleoambientes y evolución geomorfológica en yacimientos arqueológicos del sector oriental de la Depresión del Ebro durante el Holoceno superior. In: Pérez Alberti A, Martini P, Chesworth W, Martínez Cortizas A (coord) Dinámica y Evolución de medios Cuaternarios. Xunta de Galicia, Santiago de Compostela, pp. 63-80
50. Peña Monné JL, Rodanés JM (1993) Evolución geomorfológica y ocupación humana en el cerro de Masada de Ratón (Baix Cinca, prov. de Huesca). Cuaternario y Geomorfología 6:81-89
51. Peña-Monné JL, Rubio-Fernández V, Sampietro-Vattuone MM, García Giménez R (2019) Relict slopes and palaeovalleys at Taracena-Guadalajara (Central Spain): Geomorphological and palaeogeographical interpretation. Palaeogeography, Palaeoclimatology, Palaeoecology 540:106855. https://doi.org/10.1016/j.yebeh.2019.106855
52. Peña-Monné JL, Echeverría MT, Chueca J, Julián A (2000) Processus d´accumulation et d´incision pendant l´Antiquité Classique dans la vallée de la Huerva (Bassin de l´Ebre, Espagne). In: Vermeulen F (ed) Geoarchaeology of the Landscapes of Classical Antiquity. Editorial Peters, Leuven, pp. 151-159
53. Peña Monné JL, Julián A, Chueca J, Echeverría MT, Ángeles G (2004) Etapas de evolución holocena en el valle del río Huerva: Geomorfología y Geoarqueología. In: Peña-Monné JL (eds) Geografía Física de Aragón. Aspectos generales y temáticos. Univ. Zaragoza e Inst. Fernando el Católico, Zaragoza, pp. 289-302
54. Peña Monné JL, Sampietro Vattuone MM, Longares Aladrén LA, Pérez Lambán JV, Sánchez Fabre M, Alcolea Gracia M, Vallés L, Echeverría MT, Baraza C (2018) Holocene alluvial sequence of Valderazagoza (Los Monegros) in the paleoenvironmental context of the Ebro Basin (Spain). Geographical Research Letters 44 (1):321-348. http://doi.org/10.18172/cig.3358
55. Peña-Monné JL, Sampietro-Vattuone MM (2019) Late Holocene anthropic degradation records in semi-arid environments (NE Spain and NW Argentina). Geographical Research Letters 45(1):195-217. https://doi.org/10.18172/cig.3587
56. Pérez-Lambán F, Peña-Monné JL, Fanlo J, Picazo JV, Badia D, Rubio V, García-Jiménez R, Sampietro-Vattuone MM (2014) Paleoenvironmental and geoarchaeological reconstruction from late Holocene slope records (Lower Huerva Valley, Ebro Basin, NE Spain). Quaternary Research 81:1-14. http://dx.doi.org/10.1016/j.yqres.2013.10.011
57. Pérez-Rivarés FJ, Garcés M, Arenas C, Pardo G (2003) Magnetocronología de la sucesión miocena de la Sierra de Alcubierre (sector central de la cuenca del Ebro). Rev. Soc. Geol. España 15(3-4):217-231

58. Picazo Millán JV (1993) La Edad del Bronce en el Sur del Sistema Ibérico Turolense, I: Los Materiales Cerámicos. Monografías Arqueológicas del SAET, 7, Teruel.
59. Picazo Millán JV (2005) El poblamiento en el valle medio del Ebro durante la Prehistoria reciente: zonas y procesos. Revista d´Arqueologia de Ponent 15:99-117.
60. Quirantes J (1978) Estudio sedimentológico del Terciario continental de los Monegros. Institución Fernando el Católico, Zaragoza
61. Ramírez JI, Solá Subiranas J (1990) Mapa Geológico de España serie MAGNA escala 1:50000, hoja 386, Peñalba. I.G.M.E., Madrid
62. Rodríguez-Ochoa R, Olarieta JR, Santana A, Castañeda C, Calle M, Rhodes E, Bartolomé M, Peña-Monné JL, Sancho C (2019) Relict periglacial soils on Quaternary terraces in the Central Ebro Basin (NE Spain). Permafrost and Periglacial Processes 30(4):364-373. http://doi.org/10.1002/ppp.2005
63. Salazar A, Hernández-Samaniego A (1990) Mapa Geológico de España serie MAGNA escala 1:50000, hoja 357 Sariñena. I.G.M.E., Madrid.
64. Sancho C, Gutiérrez M, Peña JL, Burillo F (1988) A quantitative approach to cliff retreat starting from triangular slope facets, central Ebro Basin, Spain. Catena Supplement 13:139-146.
65. Sancho C, Meléndez A (1992) Génesis y significado ambiental de los caliches pleistocenos de la región del Cinca (Depresión del Ebro). Rev. Soc. Geol. España 5:81-93.
66. Schmidt KH (1994) Hillslopes as evidence of climatic change. In: Abrahams AD, Parsons AJ (eds) Geomorphology of desert environments. Chapman & Hall, London, pp. 553-570
67. Sheeland CE, Ward DJ (2018) Late Pleistocene talus flatiron below yhe Coal Clift cuesta, Utah, USA. Earth Surface Processes and Landforms 43(9):1973-1992. https://doi.org/10.1002/esp.4369
68. Sirvent J, Desir G, Gutierrez M, Sancho C, Benito G (1997) Erosion rates in badland areas recorded by collectors, erosion pins and profilometer techniques (Ebro Basin, NE-Spain). Geomorphology 18:61-75

# Tables

**Table 1.** Radiocarbon datings.

| sample | lab code | Age yr BP | Age cal BP | | Age cal BC/AD | | Sampled material |
|---|---|---|---|---|---|---|---|
| | | | 1 σ | 2 σ | 1 σ | 2 σ | |
| JUB-1 | D-AMS 041195 | 3252 ± 24 | 3484-3410 | 3557-3395 | 2535-1461 BC | 1608-1446 BC | Charcoal |

# Figures

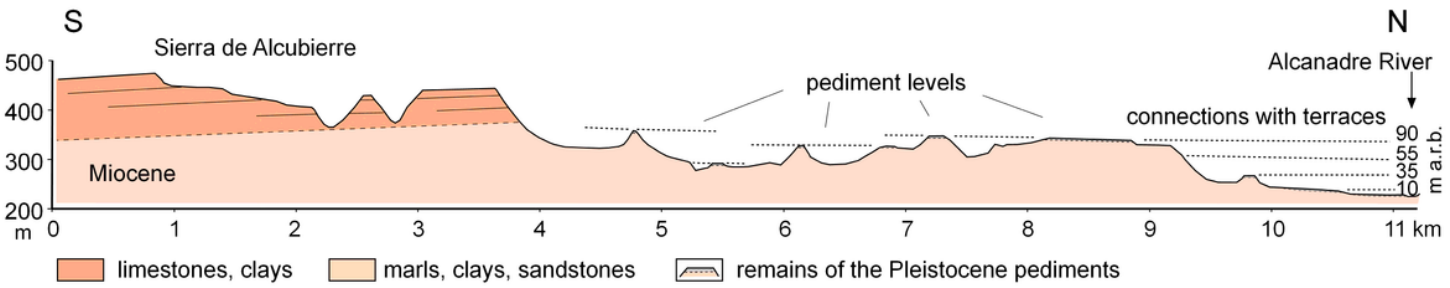


## Figure 1

Location map of Jubierre area, in the central sector of the Ebro depression, and the hills (*tozales*) analysed.

## Figure 2

Geomorphological and geological map from Jubierre area.

## Figure 3

Images of Jubierre area at different scales: (a) valleys descending from the upper limestone scarps of Jubierre; (b) aerial view of the residual hills of Los Pedregales; (c) stratigraphy of Sierra de Pallaruelo-Monte de Sora Fm on LPN hill; (d) coloured marls and clays of the LPS hill; (e) Solitario 1 hill; (f) silty alluvial fans at the foot of the hills, arranged as steps and with superficial cracking and biological soil crusts; (g) detail of popcorns and rills developed on clays and marls; (h) soil crusts on erosion processes with pedestal morphologies.

## Figure 4

DEM and orthoimage obtained from UAV flights for LPN and LPS.

## Figure 5

Detailed geomorphological map of LPN hill and general references. Marginal numbers indicate the cross-section of Fig. 6b.

## Figure 6

(a) General aerial view of LPN hill and the S2 and S3 talus flatirons set; (b) and cross-section showing the arrangement of the different slope stages; (c) location of several Bronze Age potsherds on S2 talus; (d) detail of three ceramic fragments interbedded in S2 stage.

## Figure 7

(a) Detailed geomorphological map of the LPS hill. References are the same of Fig. 5. Marginal numbers indicate the cross-section locations; (b) and (c) cross-sections of LPS hill showing the talus flatirons stages.

## Figure 8

(a) Aerial view of LPS with preserved talus slope; (b) S2 outcrop after archaeological inspection and clearing with layers indicated, location of the $^{14}C$ sample and potsherds; (c) Bronze Age potsherds from S2 talus.

## Figure 9

(a) Geormophological interpretation of Solitario 1 hill from oblique UVA photograph and location of the Fig. 9c (red circle); (b) cross-section across Solitario 1 hill as indicated on Fig. 9a; (c) talus flatiron S2 and location of the Bronze Age potsherds (red circle), one of them showed on (d).


## Figure 10

(a) Geormophological interpretation of Solitario 2 hill from oblique sUVA photograph and location of the Fig. 10c (red circle); (b) cross-section of Solitario 2 hill as indicated on Fig. 10a; (c) talus flatiron S2 and location of the Bronze Age potsherds (red circle), one of them showed on (d).

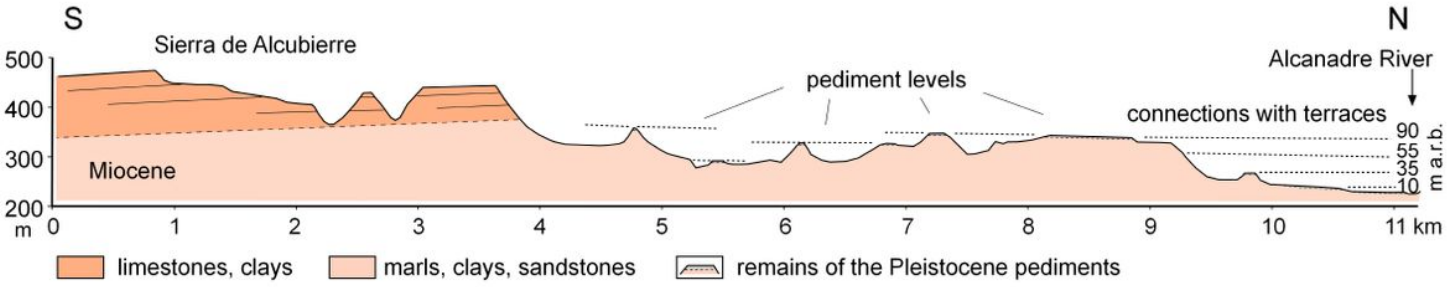


## Figure 11

(a) Topographic cross-section of the Jubierre reliefs from the upper limestone platforms (Sierra de Alcubierre) up to the Alcanadre River with the reconstruction of the pediment levels.

## Figure 12

General evolution of the Jubierre hills: (a) Initial mesa with detritic caprock (Pleistocene pediment) and S4 slope formation; (b) upper caprock retreat and S3 slope stabilization; (c) S2 slope formation and Bronze Age occupation; (d) erosion of the upper detrital caprock and marls exposure; (e) S1 slope formation, and present evolution of residual hills.

## Figure 13

Interpretation of the type of hills from Jubierre organized on three main groups according to their evolutionary stage. Explanation on the text.